

Motion-encoded dose calculation through fluence/sinogram modification

Weiguo Lu^{a)}

TomoTherapy Inc., 1240 Deming Way, Madison, Wisconsin 53717

Gustavo H. Olivera and Thomas R. Mackie

TomoTherapy Inc., 1240 Deming Way, Madison, Wisconsin 53717

and University of Wisconsin-Madison, 1300 University Avenue, Madison, Wisconsin, 53705

(Received 25 May 2004; revised 27 September 2004; accepted for publication 19 October 2004; published 17 December 2004)

Conventional radiotherapy treatment planning systems rely on a static computed tomography (CT) image for planning and evaluation. Intra/inter-fraction patient motions may result in significant differences between the planned and the delivered dose. In this paper, we develop a method to incorporate the knowledge of intra/inter-fraction patient motion directly into the dose calculation. By decomposing the motion into a parallel (to beam direction) component and perpendicular (to beam direction) component, we show that the motion effects can be accounted for by simply modifying the fluence distribution (sinogram). After such modification, dose calculation is the same as those based on a static planning image. This method is superior to the “dose-convolution” method because it is not based on “shift invariant” assumption. Therefore, it deals with material heterogeneity and surface curvature very well. We test our method using extensive simulations, which include four phantoms, four motion patterns, and three plan beams. We compare our method with the “dose-convolution” and the “stochastic simulation” methods (gold standard). As for the homogeneous flat surface phantom, our method has similar accuracy as the “dose-convolution” method. As for all other phantoms, our method outperforms the “dose-convolution.” The maximum motion encoded dose calculation error using our method is within 4% of the gold standard. It is shown that a treatment planning system that is based on “motion-encoded dose calculation” can incorporate random and systematic motion errors in a very simple fashion. Under this approximation, in principle, a planning target volume definition is not required, since it already accounts for the intra/inter-fraction motion variations and it automatically optimizes the cumulative dose rather than the single fraction dose. © 2005 American Association of Physicists in Medicine.

[DOI: 10.1118/1.1829402]

Key words: motion, dose calculation, fluence-modification

I. INTRODUCTION

Most of the radiotherapy treatment systems are based on a static patient model, which relies on a single static planning computed tomography (CT) image for treatment planning and evaluation. While in reality, patients move intrafractionally as well as interfractionally. Conventional methods of adding a margin around the clinical target volume (CTV) to get a planning target volume (PTV)^{1,2} have some known theoretical and practical problems.³ Some of these problems are (1) The PTV only addresses uncertainty in the position of the CTV, however, the uncertainty in the position of critical structures must be addressed as well.¹ (2) Motion uncertainty is most likely a probability distribution, and a simple hard margin is not sufficient.⁴ (3) PTV based treatment planning requires a uniform dose for the whole PTV and a high dose gradient along the edge of the PTV. Such requirement may not be clinically appropriate since the CTV may only have a very small chance to reach the margin of the PTV but in other cases it may extend beyond the PTV. (4) The planning dose is still a single fraction static dose while the delivered dose is actually a multifraction accumulated “motion” dose. These problems may result in significant differences between

the planned dose and the delivered dose. In addition, the process of outlining the margins on the planning workstation is not trivial.

On the other hand, very often we have some knowledge of patient motion,⁵ such as, interfraction systematic and random patient setup errors,⁶ intrafraction patient breathing variations, even the complete knowledge of time dependent motion function that is derived from a breathing control system,⁷ or other techniques.⁸ Such known motion information could be incorporated into the dose calculation for planning and evaluation.^{9,10} When the motion information is incorporated into the dose calculation, the need for the PTV may be alleviated or even eliminated. Some authors have proposed methods to account for the geometric uncertainty in dose calculation.¹¹ The most common approach was to post-process the “static” planned dose distribution^{12–15} by convolving it with a probability density function (PDF) that describes the motion uncertainty. We call this method the “dose-convolution” method. Note that the “dose-convolution” method should not be confused with the “convolution/superposition” dose calculation method. The latter is a method to calculate a static dose distribution, while the former is used to compensate motion effect. One assumption

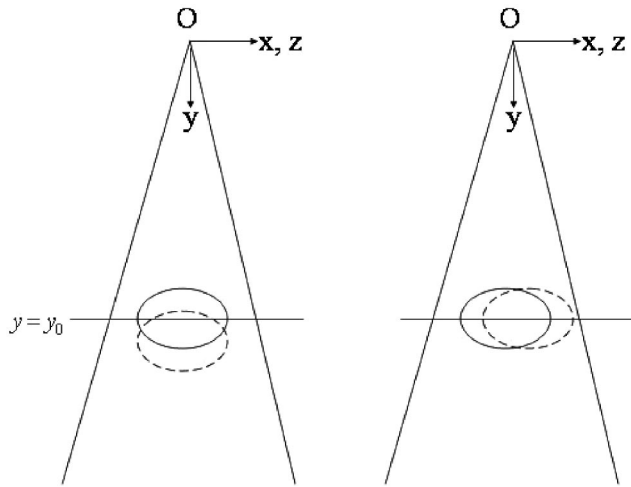


FIG. 1. Illustration of coordinate system and patient motion model. The fan beam originates at position $O(0, 0, 0)$, with direction $(0, 1, 0)$. The ellipse stands for a patient body. The left panel demonstrates the parallel (to beam direction) motion component. The right panel shows the perpendicular (to beam direction) motion component.

tion of the “dose-convolution” method is a shift invariant system,³ which implies that the shift of the patient position relative to the treatment beams results in the delivered dose being shifted with the same magnitude in the opposite direction. The conditions for such an assumption are tissue homogeneity and flat patient surface. In practice, both conditions are hardly met. The tissue heterogeneities and patient surface curvature result in potential different dose distribution shape for any beam offset position, which in turn results in an estimated dose that is different from the delivered dose. Investigations to quantify the errors in the “dose-convolution” method due to the violation of shift invariance were reported.³ But correction of such errors is difficult because it is highly patient dependent.

In this paper, instead of post-processing the static dose distribution, we develop a simple method to incorporate motion information. This method directly operates on the fluence map, or so-called sinogram in tomotherapy.^{16,17} We call this method the “fluence-modification” method. The major contributions of the “fluence-modification” method are as follows:

- (1) The “fluence-modification” method is patient independent. Therefore, it can deal with any tissue heterogeneities and surface curvature.
- (2) It models parallel (to beam direction) motion as well as perpendicular (to beam direction) motion, while the “dose-convolution” method can only model perpendicular variations.
- (3) It does not require extra calculation time for the complicated IMRT/TomoTherapy plan dose calculation. After modifying the input fluence distribution/sinogram, any standard dose calculation methods,^{18,19} such as pencil beam dose calculation,^{20,21} convolution/superposition,^{22,23} or Monte Carlo dose calculation²⁴ could be used.

II. THEORY

Given the coordinate system as illustrated in Fig. 1, let the radiation beam originate at position $(0,0,0)$ with direction $(0,1,0)$. Suppose the fluence (without attenuation by the patient body) be $S(x, y_0, z) \propto 1/(x^2 + y_0^2 + z^2)$ at plane $y = y_0$, where y_0 is the source-axis distance (Fig 1). Let $B(\mathbf{r}; x, y_0, z)$ be the dose contribution to point \mathbf{r} from a unit beamlet centered at position (x, y_0, z) . If patient is static, then the dose to point \mathbf{r} is

$$d^0(\mathbf{r}) = \int_{x,z} B(\mathbf{r}; x, y_0, z) S(x, y_0, z) dx dz. \quad (1)$$

Here $S(x, y_0, z)$ is the static fluence distribution of a radiation beam. $S(x, y_0, z)$ could be intensity modulated. The superscript 0 stands for “static” calculation.

A. Dose-convolution method

The dose-convolution method assumes a “shift invariant” system, that is, shifting patient position relative to the treatment beams results in the delivered dose being shifted in the same magnitude in the opposite direction. Such an assumption is valid only when the patient’s shift is perpendicular to beam direction, plus that patient’s body is tissue homogeneous with a flat surface. Based on such an assumption, now suppose patient has shift $\mathbf{u}_\perp = (u_x, 0, u_z)$ that is perpendicular to the y axis. The dose distribution after patient offset is

$$d^u(\mathbf{r}) = d^0(\mathbf{r} - \mathbf{u}_\perp). \quad (2)$$

If the patient has a setup variation $p(\mathbf{u})$ rather than a simple shift, then the dose distribution becomes

$$D(r) = (d^0 \otimes p)(r). \quad (3)$$

Equation (3) is the basis for the “dose-convolution” method, where \otimes stands for convolution.

B. Fluence-modification method

1. Dose calculation accounting for simple patient shift

Now suppose patient has an arbitrary small shift $\mathbf{u}(\|\mathbf{u}\| \ll y_0)$, it is equivalent to moving the source of beam by $-\mathbf{u}$ while keeping the patient in its original position.

Based on small patient motion approximation, the corresponding fluence at plane $y = y_0$ becomes

$$S^u(x, y_0, z) = \frac{x^2 + y_0^2 + z^2}{(x - u_x)^2 + (y_0 - u_y)^2 + (z - u_z)^2} \times S(x - u_x, y_0, z - u_z). \quad (4)$$

Using small beam divergence approximation, that is, $|x| < y_0, |z| < y_0$, then Eq. (4) is simplified as

$$S^u(x, y_0, z) \approx \frac{y_0^2}{(y_0 - u_y)^2} S(x - u_x, y_0, z - u_z). \quad (5)$$

The beam divergence is accounted for by the term $y_0^2/(y_0 - u_y)^2$.

The dose distribution after the patient offset is

$$d^u(\mathbf{r}) = \int_{x,z} B(\mathbf{r}; x, y_0, z) S^u(x, y_0, z) dx dz. \quad (6)$$

2. Dose calculation accounting for patient motion variations

We use a probability distribution $p(\mathbf{u})$ to describe patient motion. Here $p(\mathbf{u})$ means that the probability of offset \mathbf{u} is p .

The accumulated dose distribution due to $p(\mathbf{u})$ is

$$D(\mathbf{r}) = \int_{\mathbf{u}} d^u(\mathbf{r}) p(\mathbf{u}) d\mathbf{u}. \quad (7)$$

Insert Eq. (6) into Eq. (7), we have

$$\begin{aligned} D(\mathbf{r}) &= \int_{\mathbf{u}} \left[\int_{x,z} B(\mathbf{r}; x, y_0, z) S^u(x, y_0, z) dx dz \right] p(\mathbf{u}) d\mathbf{u} \\ &= \int_{x,z} B(\mathbf{r}; x, y_0, z) \left[\int_{\mathbf{u}} S^u(x, y_0, z) p(\mathbf{u}) d\mathbf{u} \right] dx dz \\ &= \int_{x,z} B(\mathbf{r}; x, y_0, z) S^*(x, y_0, z) dx dz, \end{aligned} \quad (8)$$

where

$$\begin{aligned} S^*(x, y_0, z) &= \int_{\mathbf{u}} S^u(x, y_0, z) p(\mathbf{u}) d\mathbf{u} \\ &= \int_{\mathbf{u}} \left(\frac{y_0}{y_0 - u_y} \right)^2 S(x - u_x, y_0, z - u_z) p(\mathbf{u}) d\mathbf{u} \end{aligned} \quad (9)$$

is called the “motion-encoded fluence.”

Suppose that $p(\mathbf{u})$ is separable into a parallel (to beam direction) component $p_{\parallel}(u_y)$ and perpendicular (to beam direction) component $p_{\perp}(u_x, u_z)$ (Fig. 1), then we have

$$\begin{aligned} S^*(x, y_0, z) &= \int_{u_y} \left(\frac{y_0}{y_0 - u_y} \right)^2 p_{\parallel}(u_y) du_y \\ &\quad \times \int_{u_x, u_z} S(x - u_x, y_0, z - u_z) p_{\perp}(u_x, u_z) du_x du_z. \end{aligned} \quad (10)$$

The first term in the right side is the contribution from the parallel component that is defined as

$$s_{\parallel} = \int_{u_y} \left(\frac{y_0}{y_0 - u_y} \right)^2 p_{\parallel}(u_y) du_y. \quad (11)$$

The second term is the contribution from the perpendicular component; it is the convolution of fluence $S(x, y_0, z)$ with the perpendicular motion function $p_{\perp}(u_x, u_z)$

$$S^*_{\perp}(x, y_0, z) = (S \otimes p_{\perp})(x, y_0, z), \quad (12)$$

where \otimes stands for convolution. Therefore, we have

$$D(\mathbf{r}) = \int_{x,z} B(\mathbf{r}; x, y_0, z) S^*(x, y_0, z) dx dz, \quad (13)$$

$$S^*(x, y_0, z) = s_{\parallel} \cdot S^*_{\perp}(x, y_0, z), \quad (14)$$

where s_{\parallel} and S^*_{\perp} are defined in Eqs. (11) and (12).

In summary, if we have some known information about patient motion, then such knowledge can be easily incorporated into dose calculation as described in Eqs. (11)–(14). Thereafter, dose calculation is similar to conventional methods, except that the beam intensities are modified in accordance with the motion information. The parallel direction modification is simply a scaling factor. The perpendicular direction modification is a simple convolution.

3. More about parallel component modification

Equation (11) describes the parallel component modification. In general, this is a correction for beam divergence. Two special cases are worth further discussions.

- (1) Symmetric parallel component motion: that is, $p_{\parallel}(u_y) = p_{\parallel}(-u_y)$, which is very common for random setup error. In this case $s_{\parallel} \approx 1$. No correction is needed.
- (2) Simple shift parallel component motion: that is, $p_{\parallel}(u_y) = \delta(u_y - \bar{u}_y)$. In this case, we have

$$s_{\parallel} = \int_{u_y} \left(\frac{y_0}{y_0 - u_y} \right)^2 \delta(u_y - \bar{u}_y) du_y = \left(\frac{y_0}{y_0 - \bar{u}_y} \right)^2. \quad (15)$$

This is a simple inverse square correction on the input fluence.

III. MATERIAL AND METHODS

A. Phantoms

We use simulated phantoms to test motion encoded dose calculations. For comparison purpose, we use the phantoms that are similar to what were used in Refs. 3 and 25. Four phantoms are created for the tests (Fig. 2). The first one (“cube-water”) is a cubic water phantom that is $20 \times 20 \times 20$ cm³ in dimension. The second one (“cube-lung”) is similar to the first one but with $7 \times 7 \times 7$ cm³ lung equivalent material (density = 0.25 g/cm³) at the center. The third one (“cylinder-water”) is a cylinder (20 cm in diameter and 20 cm long) water phantom. The fourth one (“cylinder-lung”) is similar to the third one except that there is a $7 \times 7 \times 7$ cm³ cubic lung equivalent material at the center.

B. Beams and plans

We simulate a 6 MV radiation beam that is consistent with a commercial helical TomoTherapy^{16,17,26} machine. Three plans are simulated. The first one uses a single 7×7 cm² wide beam. The second is four-field (AP/PA and two laterals) conformal plan, each field is 6.4 cm wide. The third is a 360° rotation conformal plan, which conforms to a ring target.

C. Dose calculation methods

Four different dose calculation methods that account for interfraction motion are tested and compared.



FIG. 2. Cross sections of simulated phantoms used in this paper. The left-most one is a $20 \times 20 \times 20 \text{ cm}^3$ water phantom. The second one is similar to the first one except that it has a $7 \times 7 \times 7 \text{ cm}^3$ cube lung equivalent material at center. The third one is a cylinder water phantom of 20 cm in diameter and 20 cm long. The right-most one is similar to the third one except that it has a $7 \times 7 \times 7 \text{ cm}^3$ cube lung equivalent material at center.

1. Static method

Dose calculation as performed in the conventional treatment planning system is referred to as the “static” method. This method assumes that the patient geometry does not change throughout the course of treatment. The specific dose calculation method used is the collapsed cone convolution/superposition.^{23,27}

2. Stochastic-simulation method

This method provides a “gold standard” for calculating the cumulative dose during the whole course of radiation treatment that accounts for motion variations. We use a simple Gaussian distribution to describe both the systematic and the random patient motion

$$p(u) = \frac{1}{\sqrt{2\pi}\sigma} \exp\left[-\frac{(u - \bar{u})^2}{\sigma^2}\right]. \quad (16)$$

Here the mean \bar{u} describes the systematic motion and the standard deviation σ describes the random motion. We assume that a treatment course consists of 40 fractions. We use single static plan fluence (sinogram), but assume that different fractions have different motion offsets, which are randomly sampled from a Gaussian distributed pool. A total of 40 (fraction) dose calculations are needed to evaluate this method. Each one is associated with its own shifted geometry. To calculate the cumulative dose distribution from all 40 fractions, we shift each fraction dose according to its simulated offset to map it back to the planning geometry.

3. Dose-convolution method

This method compensates the interfraction patient motion by convolving the static dose with a probability density function (PDF) describing the uncertainty. The same Gaussian distribution function (16) is used as the PDF. Only one dose calculation is needed.

4. Fluence-modification method

This is the method developed in this paper. Rather than changing the patient geometry to calculate each fraction dose, we use plan geometry only, but rather modify the

planned fluence (sinogram) in accordance with the motion information (16). Only one dose calculation is needed.

D. Interfraction motion simulation

Four types of interfraction motions are simulated. Case 1 has no motion ($\bar{u}=0, \sigma=0$). Case 2 has a 1 cm systematic motion along the lateral direction ($\bar{u}=1, \sigma=0$). Case 3 has a 1 cm (standard deviation) random motion along the lateral direction ($\bar{u}=0, \sigma=1$). Case 4 has both 1 cm systematic and 1 cm (standard deviation) random motion along lateral direction ($\bar{u}=1, \sigma=1$).

IV. RESULTS

A. Single field motion encoded dose calculation

The single field dose calculation experiment is to compare the different dose calculation methods for interfraction motion compensation. Four different methods (the “stochastic-simulation” method (gold standard), the “static” method (no compensation), the “dose-convolution” method and the “fluence modification” method) are compared. Three different kinds of interfraction motions (a 1 cm systematic lateral motion, a 1 cm (standard deviation) random lateral motion, a 1 cm systematic+1 cm (standard deviation) random lateral motion) are simulated. Four different phantoms, “cube-water,” “cube-lung,” “cylinder-water,” and “cylinder-lung” are used for tests.

Figures 3–5 illustrate the results. Figure 3 shows the results from 1 cm systematic lateral motion. Figure 4 shows results from 1 cm (standard deviation) random lateral motion. Figure 5 shows results from a combination of 1 cm systematic and 1 cm (standard deviation) random lateral motion.

For all three interfraction motion simulation cases, the “static” method (the second leftmost column) has the most significant errors. For a 1 cm systematic lateral motion, the maximum dose error is around 40% of the maximum dose. For a 1 cm standard deviation random lateral motion, the maximum dose error is around 15% of the maximum dose. For the combination of systematic and random motion, the

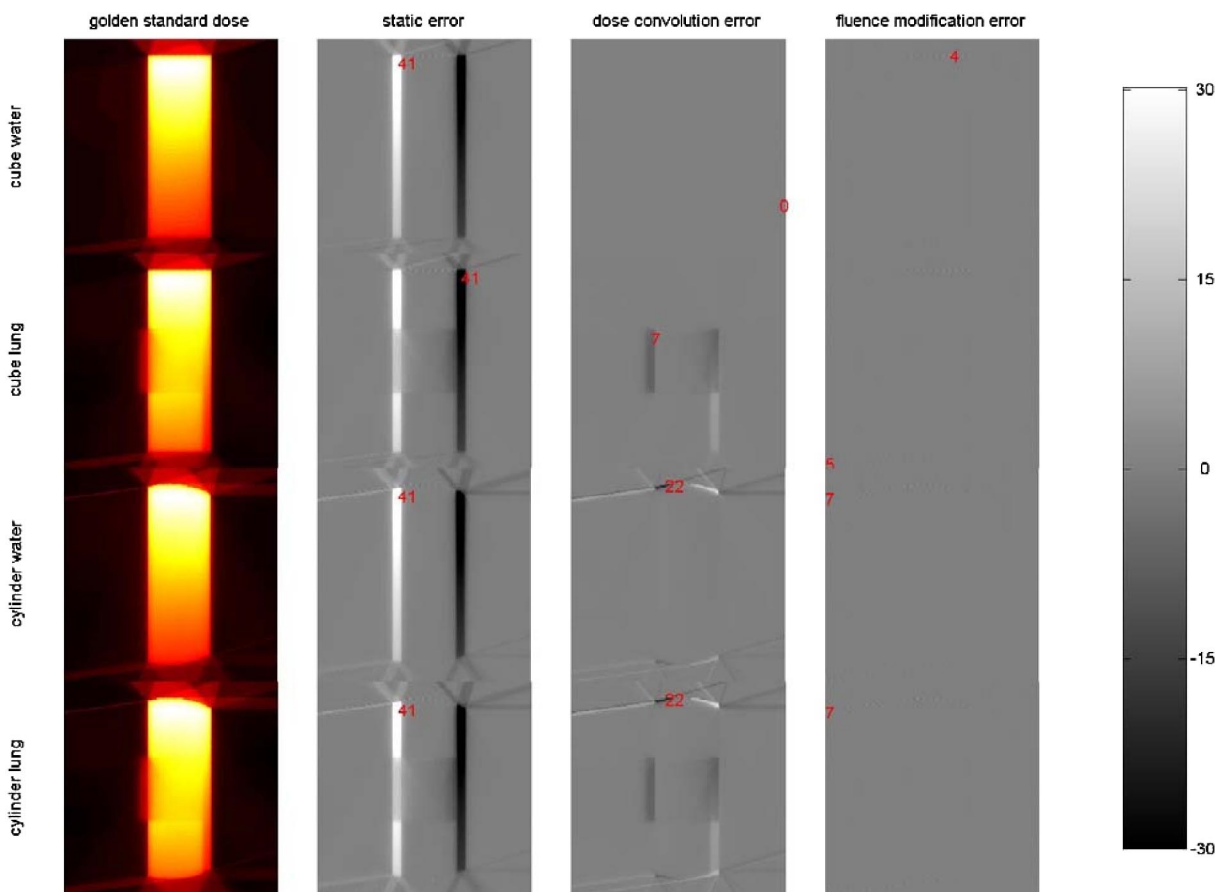


FIG. 3. Comparison of different dose calculation methods on four different phantoms with a single field. A 1 cm systematic lateral motion is used for this test. From top row to bottom row are the results from “cube-water,” “cube-lung,” “cylinder-water,” and “cylinder-lung” phantom. The left column is the dose distributions based on the “stochastic-simulation” method, which works as the “gold standard.” The second column shows the results of the dose difference between the “static” method and that of the gold standard. The third column is the dose difference between the “dose-convolution” method and the “gold standard.” The fourth column is the dose difference between the “fluence-modification” method and that of the “gold standard.” The number indicates the maximum error in the unit of percentage of the maximum dose. The rightmost color bar is the percentage difference of the maximum dose.

maximum error is around 30% of the maximum dose. The results imply that motion compensation is crucial for correct multifraction dose calculation.

For all three motion simulations studied on the “cubic-water” phantom, the maximum error in dose distribution calculated by the “dose-convolution” method (the second right-most column) is less than 5% of the maximum dose. But the errors become significant when there exists heterogeneity (“cube-lung” and “cylinder-lung”) or there is a curved surface (“cylinder-water” and “cylinder-lung”). The maximum error goes between 10% of the maximum dose for random motion case and 20% of the maximum dose for the systematic motion case. Significant errors occur in both the area-water surface region and the water-lung surface region.

For all three motion simulations studied on the “cubic-water” phantom, the “fluence-modification” method (the right-most column) is similar to the “dose-convolution” method (the second right-most column). For studies in all other three phantoms, where there exists heterogeneity (“cube-lung” and “cylinder-lung”) or a curved surface (“cylinder-water” and “cylinder-lung”), the “fluence-modification” method outperforms the “dose modification”

method. The maximum errors of the “fluence-modification” method are less than 4% of the maximum dose except for several voxels in the systematic motion case where the error reaches 7% of the maximum dose. These errors are mainly due to the limited number of samples (40) used for the “gold standard” dose calculation.²⁵

B. Conformal plan motion encoded dose calculation

Two simple conformal plans are tested in this experiment. One is a four-field plan (AP/PA and two laterals), the other is a 360° rotation conformal plan, which conforms to a ring target. The “water-cube” phantom is used for all tests. The same three motion simulations as used in the single field calculations are tested. Comparison of the “stochastic-simulation” method (gold standard) and the “fluence modification” method are performed. Note that the “fluence-modification” method only needs to calculate dose once, while the “stochastic-simulation” method requires 40 dose calculations, and each calculation requires changing the geometry and remapping the dose distribution.

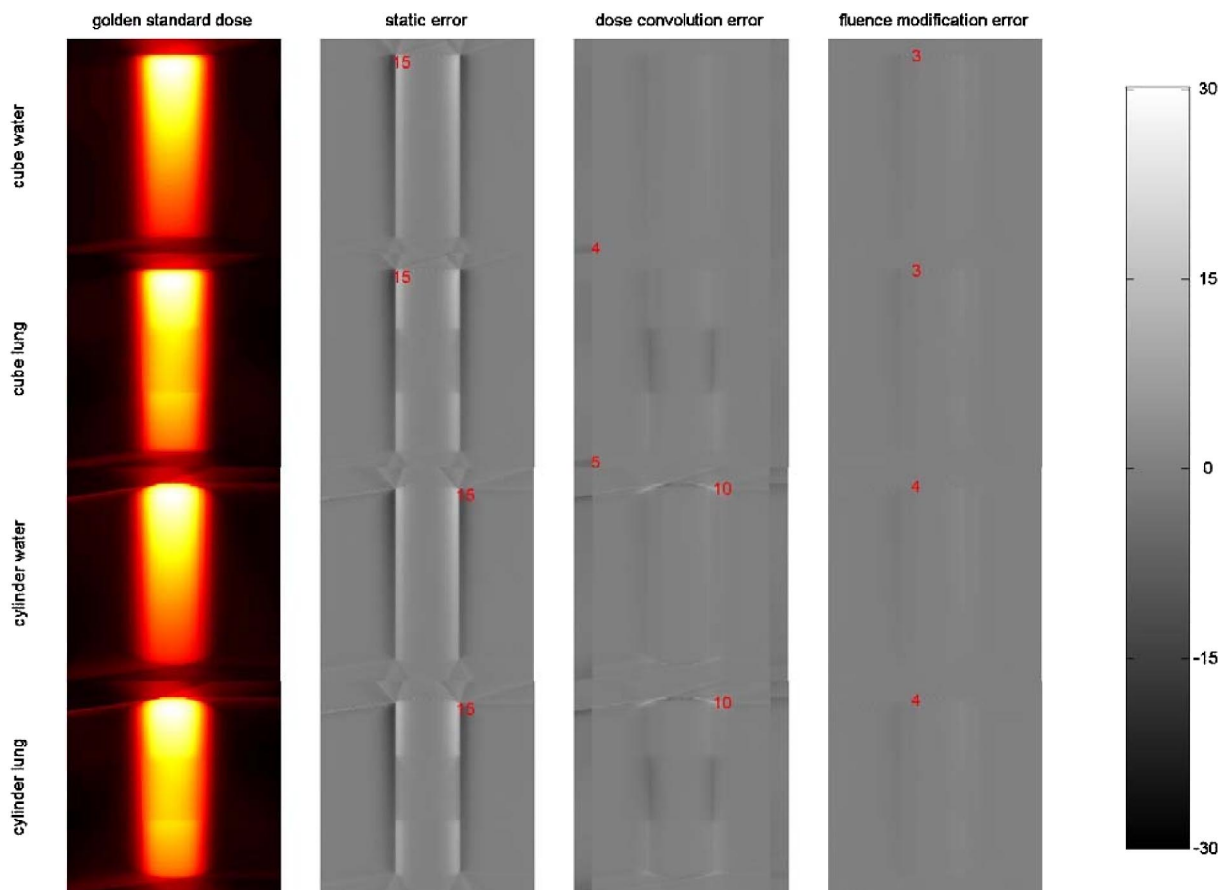


FIG. 4. Similar to Fig. 3 except that a 1 cm (standard deviation) random lateral motion is tested.

Figures 6 and 7 show the results of the four-field plan. Figure 6 shows the “motion-encoded fluence.” The left-most column shows the static plan, while the other three columns show the “motion-encoded fluence.” Note that for the lateral beam (top panel), the motion-encoded fluence is very similar to that of static plan because the motion is parallel to that direction. While for the AP/PA beam (bottom panel), which is perpendicular to the motion direction, the motion-encoded fluence is significantly different from that of the static plan. For the systematic lateral motion (the second left-most column), the “motion encoded fluence” is a simple shift of the static fluence. For the random lateral motion (the second right-most column), the “motion encoded fluence” is the blurring of the planned fluence. For the combination of systematic and random lateral motion (the right-most column), the “motion encoded fluence” has both shift and blurring. This is consistent with the motion we tested. Figure 7 compares the dose calculations based on the “fluence modification” method, which uses the “motion encoded fluences” as illustrated in Fig. 6, and the gold standard. The results show that these two methods are consistent considering the error associated with the “gold standard” dose calculation itself (limited number of samples).

Figures 8 and 9 show the results of dose calculation for the conformal rotation therapy plan on the “cylinder-water” phantom. Figure 8 shows the “motion-encoded sinogram.” A

sinogram is the projection-wised organization of fluences. Note that while the patient motion is only in the lateral direction, the motion-encoded fluences are different for different projections. This is because the contribution of perpendicular motion for different projection is different. The beams that are closest to the AP/PA direction have the maximum modifications, while the beams that are closest to lateral direction have the minimum modification. Figure 9 compares the result of dose calculation based on the “fluence-modification” method, which uses the “motion encoded sinograms” as illustrated in Fig. 8, and the gold standard. The results also show that these two methods are consistent considering the error from the “gold standard” dose calculation itself (limited number of samples).

V. DISCUSSIONS

This paper uses a small motion and small divergence approximations, which are quite reasonable in many clinical situations. When the patient motion is large and/or the beam divergence become significant, the simple “fluence modification” formula as derived in this paper will become problematic. A more complicated modification will be necessary. In any situation, we speculate that the “fluence/sinogram modification” is a relatively easy and accurate method for first order motion compensation.

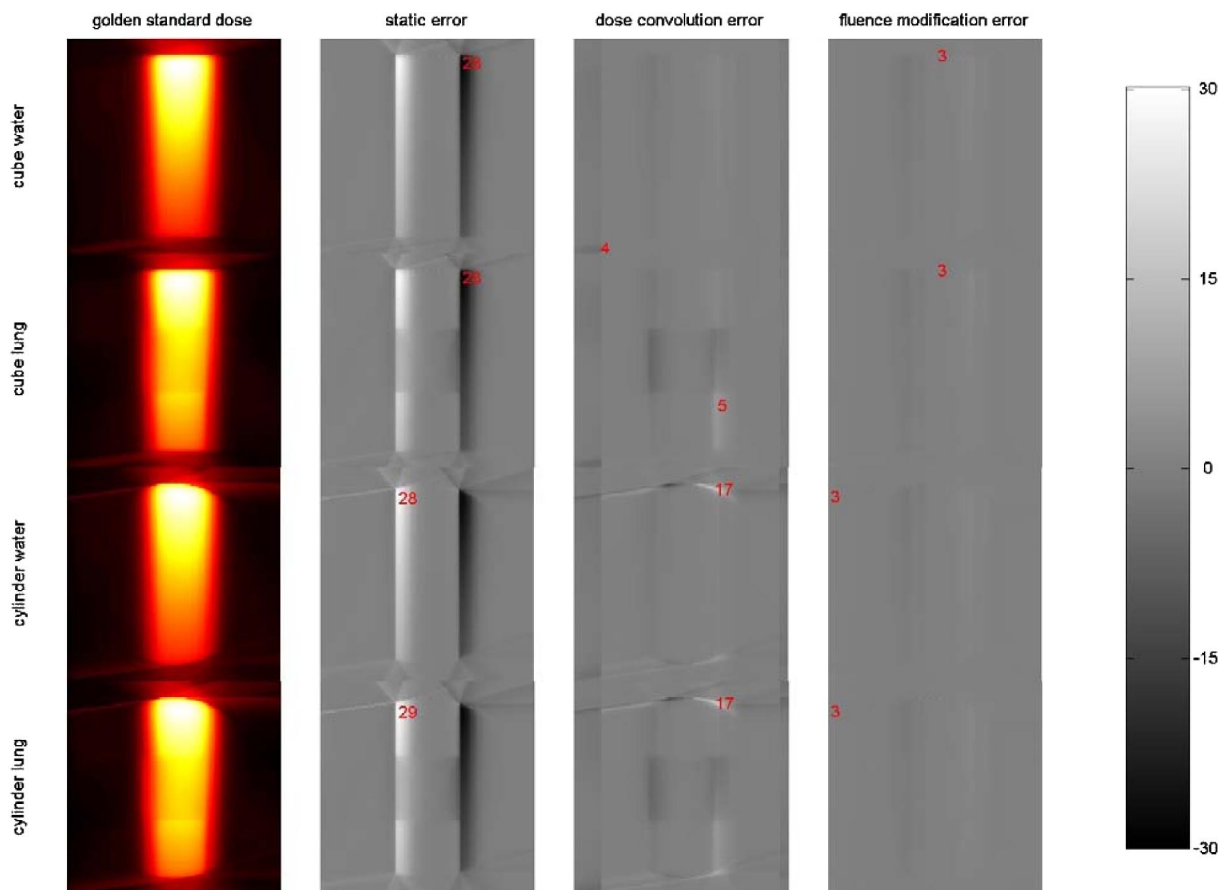


FIG. 5. Similar to Fig. 3 except that the combination of a 1 cm systematic lateral motion and 1 cm (standard deviation) random lateral motion is tested.

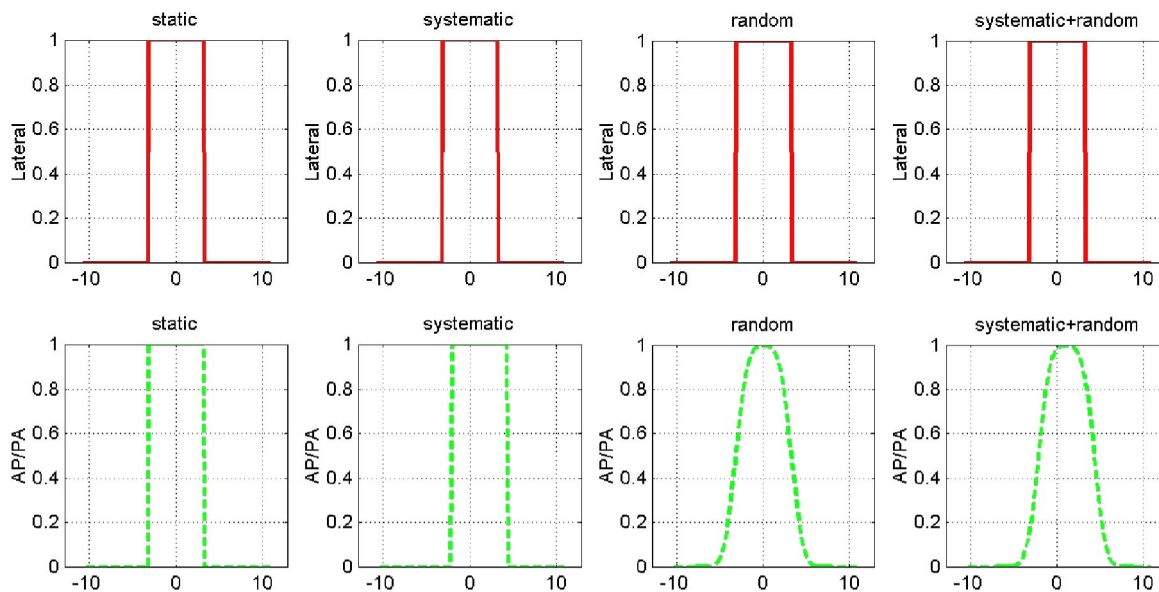


FIG. 6. "Motion encoded fluences" for the four field plan on the "cylinder-water" phantom. The left-most column is the static plan fluences. The next three columns are motion encoded fluences. The top row is the lateral fluences. The bottom row is the AP/PA fluences. From the second left column to the right, the simulated motions are systematic lateral motion (1 cm), random lateral motion (1 cm std) and systematic (1 cm)+random (1 cm std) lateral motion, respectively.

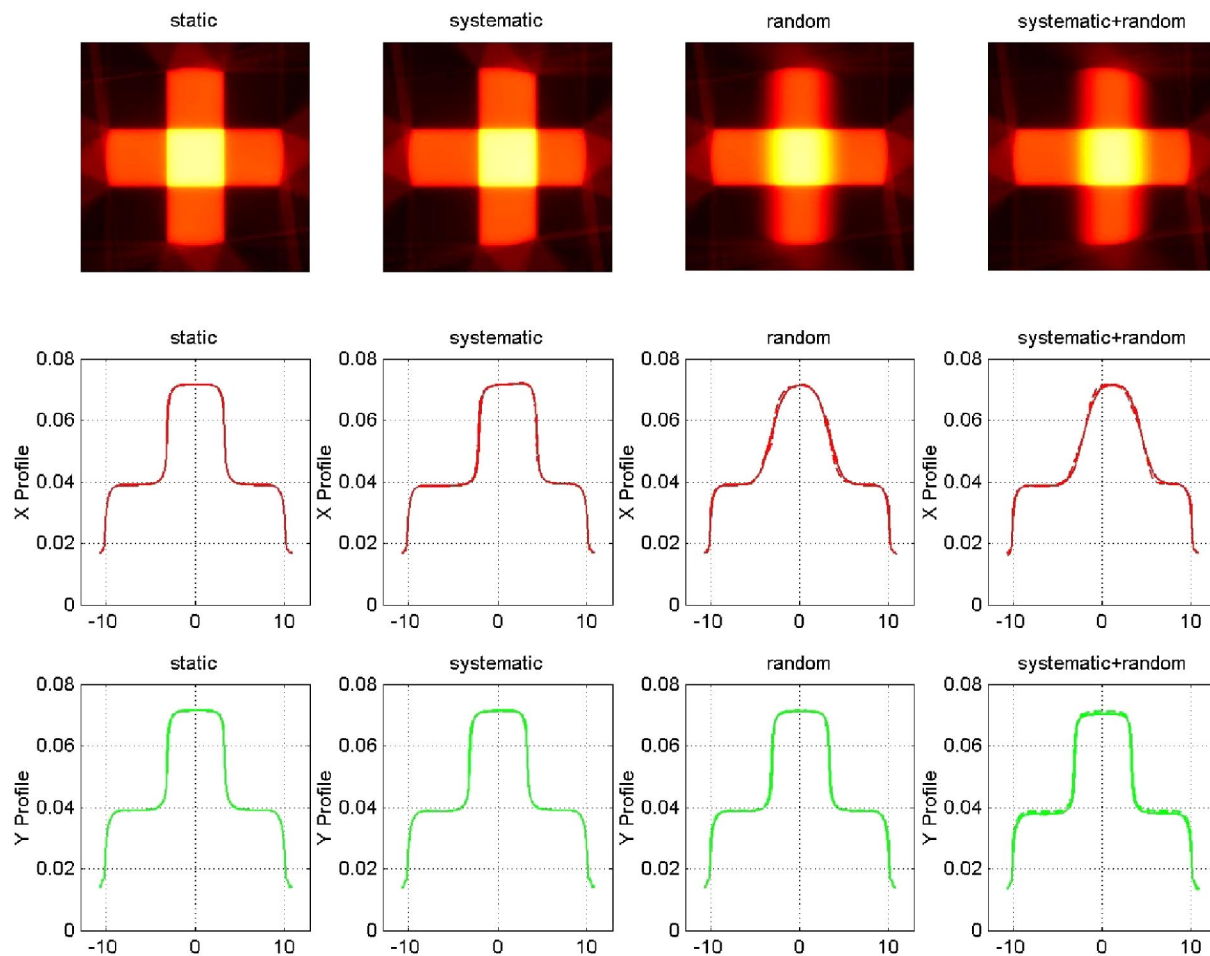


FIG. 7. Motion encoded dose calculation for the four field plan on the “cylinder-water” phantom. The top row is the dose distribution based on the “fluence-modification” method, using the “motion encoded fluences” as illustrated in Fig. 6. Panels in the middle row show the X (lateral) dose profiles. The bottom row is the Y (AP/PA) dose profiles. The solid lines are results from the “fluence-modification” method, the dash lines show results from the “stochastic-simulation” method (gold standard). From second left to right, the simulated motions are systematic lateral motion (1 cm), random lateral motion (1 cm std) and systematic (1 cm)+random (1 cm std) lateral motion, respectively.

Although we only tested the interfraction motion in this paper, the “fluence-modification” method could be applied to intrafraction motion as well. Intrafraction motion can be categorized into unpredictable motion and predictable motion. Here “predictable” means that we have knowledge about its

time dependency. Unpredictable intrafraction motion could be dealt similarly as interfraction motion. Examples of predictable intrafraction include breathing motion from a “breathing synchronized delivery” system.⁷ As for rotation therapy, we need to modify fluence for each projection in

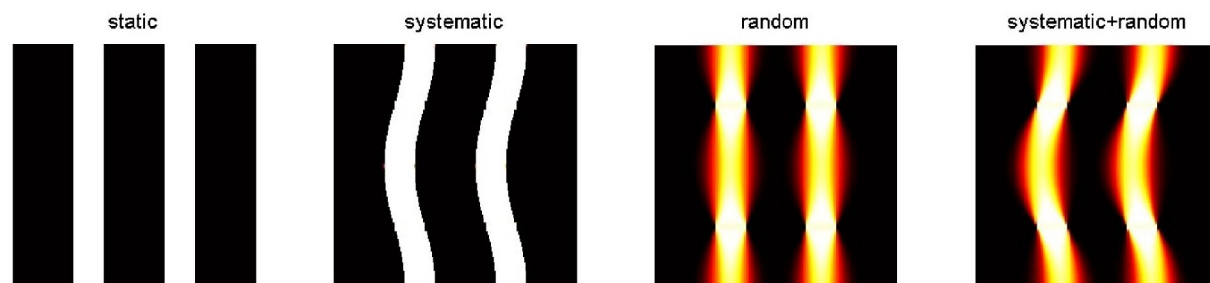


FIG. 8. “Motion encoded sinograms” for the conformal rotation therapy plan on the “cylinder-water” phantom. The left-most column is the static plan sinogram. The next three columns are motion encoded sinogram. From the second left to the right, the simulated motions are systematic lateral motion (1 cm), random lateral motion (1 cm std) and systematic (1 cm)+random (1 cm std) lateral motion.

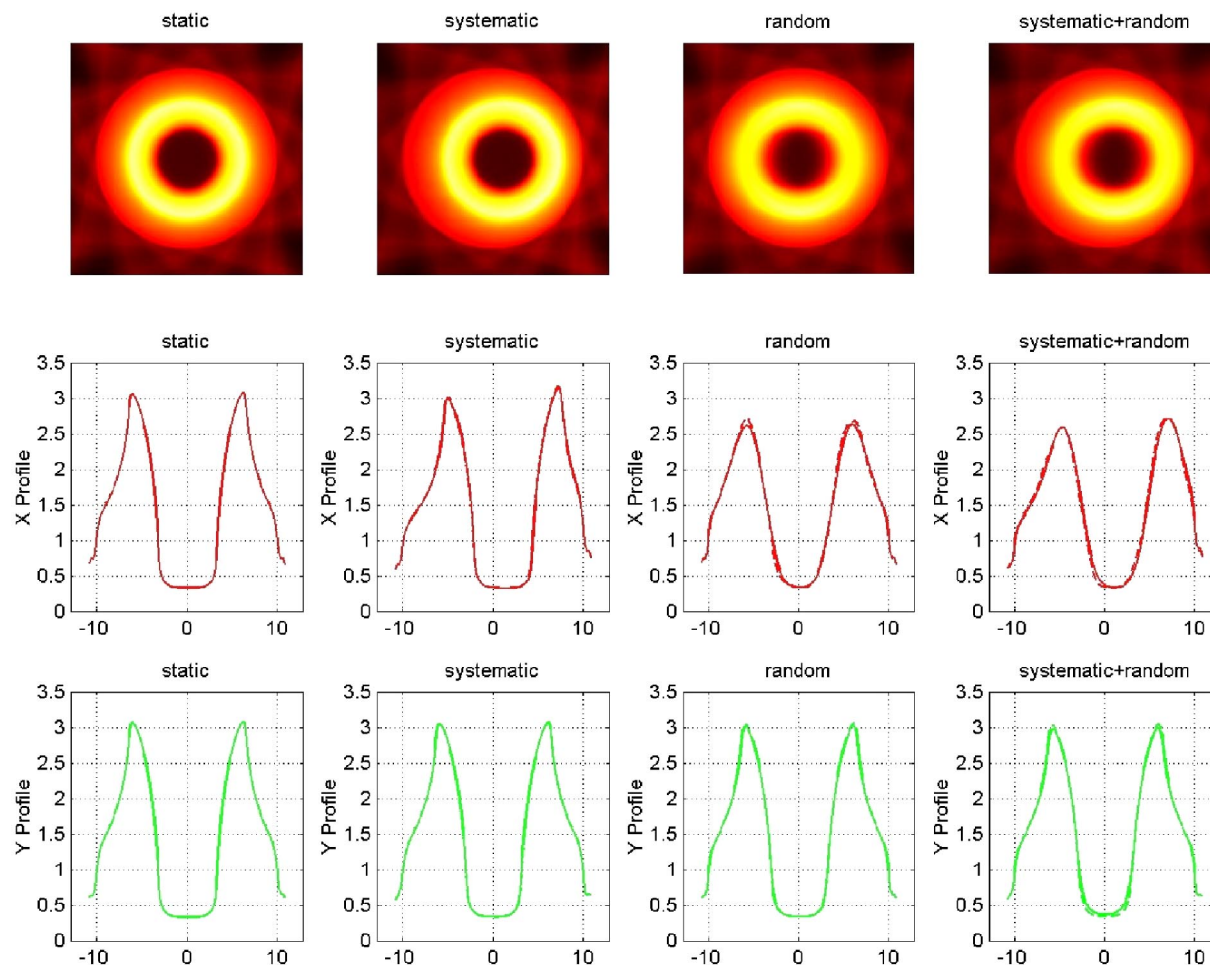


FIG. 9. Motion encoded dose calculation for conformal rotation therapy. The top row is the dose distribution based on the “fluence-modification” method, using the “motion encoded sinograms” as illustrated in Fig. 8. Panels in the middle row show the X (lateral) dose profiles. Panels in the bottom row are the Y (AP/PA) dose profiles. The solid lines are results from the “fluence-modification” method, the dashed lines show results from the “stochastic-simulation” method (gold standard).

accordance with the patient position and projection angle. The detailed investigation of intrafraction motion dose calculation will be addressed in another paper.

This paper uses a rigid-body transformation to represent patient motion. In general, patient anatomy changes are most likely deformable. We speculate that for many radiotherapy treatments, rigid-body motion is a clinically acceptable assumption for motion-encoded dose calculation. Further investigations are needed to assure this assumption. The deformable dose mapping methods^{28–31} will be under further investigation when the rigid-body assumption are not adequate to estimate the motion dose.

VI. CONCLUSION

In this paper, we present a method of motion-encoded dose calculation through fluence modification. We demonstrate that simple patient motion could be incorporated directly into dose calculation. We decompose patient motion into a parallel (to beam direction) component and perpendicular (to beam direction) component. Rather than post-processing the planned dose distribution, we account for the

motion effects by modifying fluence distribution or sinogram directly. Parallel component motion results in a simple scaling of the fluence map. While the perpendicular component motion results in a convolution of the fluence distribution with the motion distribution function. After such modification, dose calculation and optimization is the same as that with the static geometry. The developed method is superior to the “dose-convolution” method because it is not based on the “shift invariant” assumption. Therefore, it can handle heterogeneity and curvature surface very well.

We test motion-encoded dose calculation with four phantoms, four motion patterns, and three different plan beams. We compare our method with the “static” method, the “dose-convolution,” and the “stochastic-simulation” method (gold standard). As for the flat surface homogeneous phantom, our method has similar accuracy as the “dose-convolution” method. As for the heterogeneous or curved surface phantom, our method outperforms the “dose-convolution” method. The motion-encoded dose distribution using our method is within 4% of the “stochastic-simulation” method (gold standard).

Treatment sites that adhere to the conditions to apply “motion-encoded dose calculation” can in principle be done without requiring a PTV to be specified, since “motion-encoded dose calculation” already accounts for the motion variation and it automatically optimizes the accumulated dose rather than a single fraction dose. In addition, if the motion is predictable, then the resulting plan based on “motion-encoded dose calculation” can deliver the dose to the target more accurately while avoiding the sensitive structure. In both situations, neither extra optimization strategy nor extra optimization time is needed.

^aElectronic mail: wlu@tomotherapy.com

¹International Commission on Radiation Units and Measurements, “ICRU Report 50: Prescribing, recording and reporting photon beam therapy,” Bethesda, MD, 1993.

²International Commission on Radiation Units and Measurements, “ICRU Report 62: Prescribing, recording and reporting photon beam therapy, Supplement to ICRU Report 50,” Bethesda, MD, 1999.

³T. Craig, J. Battista, and J. Van Dyk, “Limitations of a convolution method for modeling geometric uncertainties in radiation therapy. I. The effect of shift invariance,” *Med. Phys.* **30**(8), 2001–2011 (2003).

⁴J. C. Stroom, H. C. J. de Boer, H. Huizenga, and A. G. Visser, “Inclusion of geometrical uncertainties in radiotherapy treatment planning by means of coverage probability,” *Int. J. Radiat. Oncol., Biol., Phys.* **43**, 905–919 (1999).

⁵W. Lu, *Motion Detection and Correction for Image Guided Radiation Therapy* (Ph.D. Thesis, University of Wisconsin-Madison, WI, 2001).

⁶P. J. Keall, W. A. Beckham, J. T. Booth, S. F. Zavgorodni, and M. Oppelaar, “A method to predict the effect of organ motion and set-up variations on treatment plans,” *Australas. Phys. Eng. Sci. Med.* **22**, 48–52 (1999).

⁷T. Zhang, H. Keller, M. O’Brien, T. R. Mackie, and B. Paliwal, “Application of the spirometer in respiratory gated radiotherapy,” *Med. Phys.* **30**, 3165–72 (2003).

⁸W. Lu and T. R. Mackie, “Tomographic motion detection and correction directly in sinogram space,” *Phys. Med. Biol.* **47**(4), 1267–1284 (2002).

⁹J. G. Li and L. Xing, “Inverse planning incorporating organ motion,” *Med. Phys.* **27**(8), 1573–1578 (2000).

¹⁰M. van Herk, P. Remeijer, and J. Lebesque, “Inclusion of geometric uncertainties in treatment plan evaluation,” *Int. J. Radiat. Oncol., Biol., Phys.* **52**, 1407–1422 (2002).

¹¹M. Goitein, “Calculation of the uncertainty in the dose delivered during radiation therapy,” *Med. Phys.* **12**, 608–612 (1985).

¹²A. Bel, M. van Herk, and J. Lebesque, “Target margins for random geometrical treatment uncertainties in conformal radiotherapy,” *Med. Phys.* **23**, 1537–1545 (1996).

¹³A. E. Lujan, E. W. Larsen, J. M. Balter, and R. K. Ten Haken, “A method for incorporating organ motion due to breathing into 3D dose calculation,” *Med. Phys.* **26**, 715–720 (1999).

¹⁴S. D. McCarter and W. A. Beckham, “Evaluation of the validity of a convolution method for incorporating tumor movement and setup variations into the radiotherapy treatment plans,” *Phys. Med. Biol.* **45**, 923–931 (2000).

¹⁵S. D. McKenzie, M. Van Herk, and B. Mijnheer, “The width of margins

in radiotherapy treatment plans,” *Phys. Med. Biol.* **45**, 3331–3342 (2000).

¹⁶T. R. Mackie, T. W. Holmes, S. Swerdloff, P. J. Reckwerdt, J. O. Deasy, J. Yang, B. Paliwal, and T. Kinsella, “Tomotherapy: A new concept for the delivery of dynamic conformal radiotherapy,” *Med. Phys.* **20**(6), 1709–1719 (1993).

¹⁷G. H. Olivera, D. M. Shepard, K. Ruchala, J. S. Aldridge, J. Kapatoes, E. E. Fitchard, P. J. Reckwerdt, G. Fang, J. Balog, J. Zachman, and T. R. Mackie, in “Tomotherapy: Modern Technology of Radiation Oncology,” edited by J. V. Dyk (Medical Physics Publishing, Madison, 1999).

¹⁸A. Ahnesjö and M. M. Aspradakis, “Review: Dose calculations for external photon beams in radiotherapy,” *Phys. Med. Biol.* **44**, R99–R155 (1999).

¹⁹T. R. Mackie, P. Reckwerdt, T. McNutt, M. Gehring, and C. Sanders, editors, “Photon beam dose computations,” *Proceedings of the 1996 Summer School for the American Association of Physicists in Medicine*, edited by T. R. Mackie and J. R. Palta (Advanced Medical Publishing, Vancouver, B.C., Canada, 1996).

²⁰R. Mohan, C. Chui, and L. Lidofsky, “Differential pencil beam dose computation modal for photons,” *Med. Phys.* **13**, 64–73 (1986).

²¹J. D. Bourland and E. L. Chaney, “A finite-size pencil beam model for photon dose calculation in three dimensions,” *Med. Phys.* **19**, 1401–1412 (1992).

²²A. Ahnesjö, “Collapsed cone convolution of radiant energy for photon dose calculation in heterogeneous media,” *Med. Phys.* **16**, 577–592 (1989).

²³W. Lu, G. H. Olivera, P. J. Reckwerdt, and T. R. Mackie, “Accurate convolution/superposition for multi-resolution dose calculation,” *Phys. Med. Biol.* (submitted) 2004.

²⁴P. Andero, “Monte Carlo techniques in medical radiation physics,” *Phys. Med. Biol.* **36**, 861–920 (1991).

²⁵T. Craig, J. Battista, and J. Van Dyk, “Limitations of a convolution method for modeling geometric uncertainties in radiation therapy. II. The effect of finite number of fractions,” *Med. Phys.* **30**(8), 2012–2020 (2003).

²⁶T. R. Mackie, J. Balog, K. Ruchala, D. Shepard, S. Aldridge, E. Fitchard, P. Reckwerdt, G. Olivera, T. McNutt, and M. Mehta, “Tomotherapy,” *Semin Radiat. Oncol.* **9**(1), 108–117 (1999).

²⁷G. H. Olivera, J. P. Balog, R. McDonald, W. Lu, J. Kapatoes, P. J. Reckwerdt, R. Jeraj, K. Ruchala, and T. R. Mackie, “Commissioning of collapsed cone convolution-superposition dose calculation for use in IMRT rotational deliveries,” *Med. Phys.* (to be published).

²⁸W. Lu, T. R. Mackie, H. Keller, K. J. Ruchala and G. H. Olivera, “A generalization of adaptive radiotherapy and the registration of deformable dose distribution,” in *International Conference on the use of Computers in Radiation Therapy*, XIIth ICCR, Heidelberg, Germany, edited by W. Schlegel and T. Bortfeld, 521–523 (2000).

²⁹T. Zhang, R. Jeraj, H. Keller, W. Lu, G. H. Olivera, T. R. McNutt, T. R. Mackie, and B. Paliwal, “Treatment plan optimization incorporating respiratory motion,” *Med. Phys.* **31**(6), 1576–1586 (2004).

³⁰G. H. Olivera, K. Ruchala, W. Lu, J. Kapatoes, P. Reckwerdt, R. Jeraj, and R. Mackie, “Evaluation of patient setup and plan optimization strategies based on deformable dose registration,” *Int. J. Radiat. Oncol., Biol., Phys.* **57**(2), S188–S189 (2003).

³¹W. Lu, M. Chen, G. H. Olivera, K. Ruchala, and T. R. Mackie, “Fast free-form deformable registration via calculus of variations,” *Phys. Med. Biol.* **49**, 3067–3087 (2004).